# Factors Influencing the Accuracy of Determining Tissue Physiology Quantitatively Using Optical Spectroscopy

**Janelle E. Bender, Laura K. Moore, Karthik Vishwanath, Nirmala Ramanujam**
*Department of Biomedical Engineering, Duke University, 136 Hudson Hall, Box 90281, Durham, NC 27708*
*Author e-mail address: janelle.bender@duke.edu*

**Abstract:** The accuracy of quantifying optical properties using optical spectroscopy and a Monte Carlo model of light transport was assessed. We show accurate extractions from single and multi-absorber phantoms, independent of probe and instrument.

**OCIS codes:** (170.4580) Optical diagnostics for medicine; (170.6510) Spectroscopy, tissue diagnostics; (160.4760) Optical properties

## 1. Introduction

Diffuse reflectance spectroscopy in the ultraviolet-visible (UV-VIS) range can be used to quantitatively measure tissue physiological parameters non-invasively and *in vivo*. An inverse Monte Carlo model of light transport [1] developed by our group has been used to extract optical scattering and absorption from both tissue-simulating phantoms and biological tissues *ex vivo* [2]. In the inverse Monte Carlo model, the code iteratively updates the optical properties associated with the measured signal until the sum of squares error between measured and Monte Carlo-modeled diffuse reflectance is minimized. We calibrate by a reference phantom, which enables the measured and Monte Carlo signal to be on the same scale. The choice of reference phantom can impact the accuracy of the extracted optical properties, and so it is crucial to test the effect of different references.

Additionally, clinical diffuse reflectance measurements can be made using different instruments, fiber-optic probes, and instrument-specific settings. Here we assess the effect of different probes, instruments, and reference phantoms on the accuracy of quantifying extracted optical absorption and scattering from the Monte Carlo model.

## 2. Methods

### 2.1. Instruments and probes

We conducted a series of phantom studies using two instruments and probes. Instrument A consisted of a 450 W Xenon (Xe) Arc lamp (JY Horiba), a scanning double-excitation monochromator (Gemini 180, JY Horiba), an imaging spectrograph (Triax 320, JY Horiba), and a CCD camera (CCD3000, JY Horiba). Instrument B (SkinSkan, JY Horiba) consisted of a 150 W Xe Arc lamp, double-grating excitation, emission monochromators, and an extended red photomultiplier tube (PMT) (Fig. 1a). A laptop computer controlled the instruments.

The illumination and collection light was coupled through one of two bifurcated probes (Fig. 1b). Probe A (Romack) had a 19-fiber illumination core surrounded by an 18-fiber collection ring, both with 0.22 NA. Probe B (Romack) consisted of 29 active illumination fibers arranged around 29 collection fibers, with respective NAs of 0.125 and 0.12. The core/cladding diameter of both Probe A and Probe B was 200/245 μm.

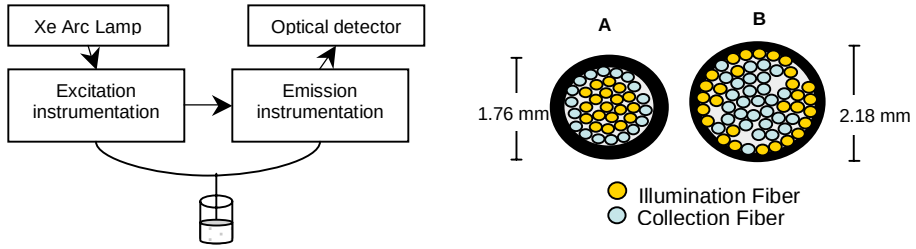


**Fig. 1. (a) Generalized schematic of the instruments used; (b) Schematic of probes A and B**

### 2.2. Phantom composition

Phantoms were composed of 1 μm diameter polystyrene spheres (07310, Polysciences, Inc.) as the scatterer and hemoglobin (H0267, Sigma Co.) and/or crocin (17304, Fluka) as the absorber. Hemoglobin (Hb) and crocin were chosen as the absorbers, because two of the absorbers in breast tumors are blood (Hb) and beta carotene (similar absorbance as crocin) [3]. The phantoms were designed to mimic the absorption and scattering levels of human breast tissue in the UV-VIS range [4].

Four sets of phantoms were tested: (1) Hb additions in an Hb-sphere phantom, (2) sphere additions in an Hb-sphere phantom, (3) crocin additions in a crocin-sphere phantom, and (4) crocin additions in a crocin-Hb-sphere phantom. Set 1 (Table 1) consisted of 10 phantoms with five absorber levels and one of two scattering levels (S1 and S2), and set 2 (Table 2) consisted of 10 phantoms with five scattering levels and one of two absorber levels (A1 and A2). For set 1, Hb was added to create the five absorber levels, while for set 2, spheres were added to create the five scattering levels. The addition of absorber or scatterer caused a dilution effect and thus a decrease in $\mu_s'$ for set 1 or a decrease in $\mu_a$ for set 2, as shown in the tables. For set 3, the same two scattering levels from set 1 were used, and the range of $\mu_a$ for crocin was similar to the levels in set 1 and 2. Phantom set 4 had optical properties that were a subset of these three sets.

**Table 1: Levels of $\mu_a$ and $\mu_s$' for phantom set 1; average was taken over 350-600 nm**

| **Absorber levels** | | **Scatterer levels** | | | |
|---|---|---|---|---|---|
| | | **S1** | | **S2** | |
| $\mu_a$ range($cm^{-1}$) | Mean $\mu_a$($cm^{-1}$) | $\mu_s$' range($cm^{-1}$) | Mean $\mu_s$'($cm^{-1}$) | $\mu_s$' range($cm^{-1}$) | Mean $\mu_s$'($cm^{-1}$) |
| 0.01 - 0.79 | 0.2 | 11.1 - 16.4 | 14.8 | 18.5 - 27.5 | 24.6 |
| 0.08 - 7.0 | 1.6 | 10.5 - 15.6 | 14 | 17.6 - 26.1 | 23.4 |
| 0.11 - 10.2 | 2.3 | 10.2 - 15.2 | 13.6 | 17.1 - 25.4 | 22.8 |
| 0.14 - 12.6 | 2.8 | 10.0 - 14.9 | 13.4 | 16.8 - 24.9 | 22.3 |
| 0.17 - 15.7 | 3.6 | 9.7 - 14.5 | 13 | 16.3 - 24.2 | 21.7 |

**Table 2: Levels of $\mu_a$ and $\mu_s$' for phantom set 2; average was taken over 350-600 nm**

| **Absorber levels** | | | | **Scatterer levels** | |
|---|---|---|---|---|---|
| **A1** | | **A2** | | | |
| $\mu_a$ range($cm^{-1}$) | Mean $\mu_a$($cm^{-1}$) | $\mu_a$ range($cm^{-1}$) | Mean $\mu_a$($cm^{-1}$) | $\mu_s$' range($cm^{-1}$) | Mean $\mu_s$'($cm^{-1}$) |
| 0.12 - 7.7 | 1.7 | 0.21 - 13.6 | 3 | 7.5 - 11.0 | 9.9 |
| 0.11 - 7.3 | 1.6 | 0.20 - 12.9 | 2.8 | 11.2 - 16.4 | 14.8 |
| 0.11 - 6.9 | 1.5 | 0.19 - 12.2 | 2.7 | 15.0 - 22.0 | 19.7 |
| 0.10 - 6.5 | 1.4 | 0.18 - 11.5 | 2.5 | 18.6 - 27.3 | 26.6 |
| 0.09 - 6.1 | 1.3 | 0.17 - 10.8 | 2.3 | 22.5 - 33.0 | 29.6 |

### 2.3. Reference phantom

To model what is done in the clinic, we tested the quantitative accuracy of extracting the concentration of absorbers in the multi-absorber phantom set 4 when the reflectance was calibrated to reference phantoms from a single-absorber phantom set measured on a different day.

## 3. Results

### 3.1. Instrumentation and probe-specific

Phantom set 1 was used to compare measurements taken under 2.5 nm and 10 nm spectral bandpass settings on Instrument A. The bandpass was varied by using either a 600 grooves/mm grating blazed at 400 nm or a 300 grooves/mm grating blazed at 500 nm in the imaging spectrograph. Errors were averaged over all reference-target phantom combinations. The extraction of $\mu_a$ was significantly better ($p=0.004$) for phantoms measured with the 2.5 nm bandpass (Table 3).

**Table 3: Average percent errors for instrumentation factors**

| | **Spectral Bandpass** | |
|---|---|---|
| | *2.5 nm BP* | *10 nm BP* |
| Mean error in $\mu_a$ (%) | 9.87 ± 4.60 | 31.98 ± 20.41 |
| Mean error in $\mu_s$' (%) | 5.82 ± 2.77 | 3.91 ± 1.69 |

Phantom sets 1 and 2 were tested using Probe A and both instruments. The average percent errors were taken over the four reference phantoms common to set 1 and 2 (A1 S1, A1 S2, A2 S1, A2 S2). Instrument B did significantly better ($p=0.0002$) than Instrument A in extracting $\mu_a$ for phantom set 2. The same phantom sets were tested using Instrument B and both probes. Probe A did significantly better ($p=0.003$) than Probe B in extracting $\mu_a$ for phantom set 2. Table 4 summarizes the extracted errors for these experiments. Although we saw an advantage with Instrument B and Probe A, we are confident that the errors for all instrument-probe combinations are sufficiently low to state the model extracts accurate properties independent of instrument and probe.

**Table 4: Average percent errors for instrument and probe experiments**

| | **Instruments** | | **Probes** | |
|---|---|---|---|---|
| | *Phantom set 1* | | | |
| | A | B | A | B |
| Mean error in $\mu_a$ (%) | 11.21 ± 3.41 | 5.61 ± 1.42 | 5.61 ± 1.42 | 2.95 ± 1.22 |
| Mean error in $\mu_s$' (%) | 5.62 ± 2.63 | 4.39 ± 1.69 | 4.39 ± 1.69 | 6.22 ± 3.38 |
| | *Phantom set 2* | | | |
| Mean error in $\mu_a$ (%) | 6.35 ± 0.29 | 3.23 ± 0.29 | 3.23 ± 0.29 | 4.88 ± 0.32 |
| Mean error in $\mu_s$' (%) | 3.41 ± 0.64 | 5.21 ± 1.14 | 5.21 ± 1.14 | 7.48 ± 1.33 |

### 3.2. Phantom-Specific

Phantom set 1 with Hb as the single absorber was compared to phantom set 3 with crocin as the single absorber for reference-target combinations with optical properties common to both sets. The concentration of the absorber was extracted accurately for either set, with average percent errors of 8.35 ± 5.27% for Hb (set 1) and 8.69 ± 0.87% for crocin (set 3). The model also performed well for the two-absorber phantoms from set 4. The extracted versus expected concentration for each absorber showed excellent agreement when normalized to all reference phantoms. The average percent error in Hb concentration was 4.97 ± 1.12%, and for crocin concentration it was 6.56 ± 2.51%.

We then tested the effect of using a single-absorber phantom measured on one day to extract optical properties from a multi-absorber phantom set measured on another day; corrections were made for daily variations in the lamp. Phantoms from set 2, with Hb as the single absorber, were used as references for the multi-absorber phantoms from set 4. The model was able to accurately extract the concentration of Hb and crocin for all reference-target combinations, by calibrating to both absorbers (Fig. 2). The solid line represents the line of perfect agreement. The correlation coefficients for Hb and crocin were 0.991 and 0.996, and the average percent error in Hb and crocin concentration was 10.48 ± 2.80% and 11.42 ± 4.77%, respectively. This extraction accuracy gives us the confidence that single-absorber phantoms can be used as references for clinical data, when calibrated to the proper absorbers.

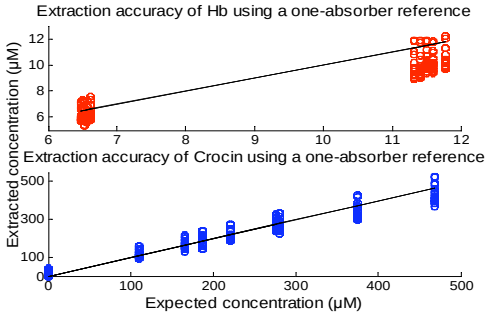


**Fig. 2: Extracted Hb (top) and crocin (bottom) when one-absorber phantoms were used as references for multi-absorber phantoms**

## 4. Discussion

We demonstrate the feasibility for our Monte Carlo model of light transport to accurately extract optical properties of multi-absorber tissue-mimicking phantoms over a wide range of wavelengths, independent of instrument and probe. Maximized quantitative accuracy can be achieved by using a narrow spectral bandpass. Furthermore, we show the ability to extract information about multi-absorber phantoms using reference phantoms consisting of only one absorber. This is directly translatable to single absorber phantoms being used as references for tissue measurements in the preclinical or clinical setting. The results from these studies give us confidence in quantifying optical properties from clinical studies.

## 5. References

[1] G. M. Palmer and N. Ramanujam, "Monte Carlo-based inverse modeling for calculating tissue optical properties. Part I: Theory and validation on solid phantoms," Appl. Optics **45,** 1062-1071 (2006).

[2] G. M. Palmer, C. Zhu, T. M. Breslin, F. Xu, K. W. Gilchrist, and N. Ramanujam, "Monte Carlo-based inverse modeling for calculating tissue optical properties. Part II: Application to breast cancer diagnosis," Appl. Optics **45,** 1072-1078 (2006).

[3] Y. Yang, E. J. Celmer, J. A. Koutcher, R. R. Alfano, "DNA and protein changes caused by disease in human breast tissues probed by the Kubelka-Munk spectral function," Photochem. Photobiol. **75,** 625-632 (2002).

[4] W. -F. Cheong, *Optical-Thermal Response of Laser-Irradiated Tissue* (Plenum 1995), Appendix to Chap. 8.